Spectral-Linewidth Studies of Pr^{3+} in Yttrium Aluminum Garnet

J. T. Gourley*
Department of Physics, Monash University, Clayton, Victoria, Australia
(Received 1 April 1971)

It has been recently shown that the variation of spectral linewidth as a function of temperature in sharp optical spectra can be adequately explained in terms of phonon-ion interactions. A detailed analysis of the $^3H_4 \rightarrow {}^3P_0$ transitions of Pr^{3+} (1%) in yttrium aluminum garnet (YAG) has allowed the analysis of the resultant line-broadening effect into its component ion-relaxation processes, each having its own temperature variation. Our results show that it is necessary to include the temperature-dependent direct phonon processes, if agreement is to be reached between the theoretical expression for the linewidth and the experimental data. In many previous studies these processes had been included only as a constant factor, independent of temperature. The coupling parameters for these transitions have been determined and are consistent with the nature of the YAG lattice.

I. INTRODUCTION

Whenever an impurity ion is placed in a host lattice there is an interaction between it and the surrounding lattice. This interaction takes two distinct forms. The first is a static interaction via the surrounding crystal field to produce a crystal-field splitting of the free-ion energy levels. The second form is a dynamic type of interaction via the surrounding phonon system which results in observable temperature-dependent effects on the optical spectrum of the ion. Such an interaction or coupling between the ion and the lattice is observed as line broadening, line shifting, or the production of vibrational sideband spectra. A study of any one of these observable effects as a function of temperature gives us valuable information concerning the strength and type of interaction taking place between the ion and its surrounding phonon system.

To determine the extent of such interactions in yttrium aluminum garnet (YAG) we chose to dope the lattice with a small amount (1%) of Pr^{3+}. Being a rare-earth ion, Pr^{3+} has narrow spectral lines at low temperatures in most compounds because of the shielded nature of the valence $4f$ shell. The resultant small interaction with the crystal-field potential means that inhomogeneous broadening, due, for example, to strains in the lattice, will be small and will allow us to freely study the temperature-dependent homogeneous line broadening. A low percentage of dopant ensures that there is no exchange of pair interactions between neighboring ions and that the lattice is not disturbed to any great extent at any particular locality. This means that each ion should have nearly identical surroundings except for any local strains in the lattice.

Pr^{3+} has an ideal electronic transition for such studies. It is the transition from the ground-state multiplet $^3H_4$ to the isolated singlet excited-state $^3P_0$ level which occurs in the visible region at about 5000 Å. Any line-broadening effects observed in these transitions must then arise from ion-relaxation mechanisms within the ground-state multiplet. The chemical substitution of Pr^{3+} for Y^{3+} provides no difficutly due to their similar physical and chemical properties. Such a substitution leads to little distortion of the lattice.

The crystal structure of the garnets is quite complicated, but from a macroscopic viewpoint the overall symmetry is that of a cubic nature. The first extensive study of the garnet structure was carried out by Yoder and Keith.[1] Geller and Gilleo[2] have since carried out a detailed study on yttrium iron garnet (YIG), $Y_3Fe_2(FeO_4)_3$. Spencer *et al.*[3] have made physical measurements on the garnets, which include acoustic wave velocities, elastic stiffness constants, and x-ray densities. In general the rare-earth ions can be pictured as being situated in distorted cubes with a point symmetry of D_2.

The crystal-field potential for YAG has been determined by Hutchings and Wolf[4] using a point-charge model and experimental data for Yb^{3+} in YAG. Using Stevens's notation[5]

$$\mathcal{H}_{\text{cryst}} = V = \sum_{k,q} V_k^q ,$$

with $k = 2,\ 4,\ 6$, and $q\ (\leq k) = 0,\ 2,\ 4,\ 6$, we have

$$V = B_2^0 \alpha O_2^0 + B_2^2 \alpha O_2^2 + B_4^0 \beta O_4^0 + B_4^2 \beta O_4^2 + B_4^4 \beta O_4^4 + B_6^0 \gamma O_6^0 + B_6^2 \gamma O_6^2 + B_6^4 \gamma O_6^4 + B_6^6 \gamma O_6^6 ,$$

where O_k^q are the angular momentum operators given by Stevens; α, β, and γ are the Stevens multiplicative constants Θ_k with $k = 2,\ 4$, and 6; and B_k^q are the crystal-field parameters $B_k^q = A_k^q \langle r^k \rangle$ tabulated by Hutchings and Wolf[4] for YAG.

In recent years several experiments have been carried out on various impurity-doped lattices to determine the extent and nature of spectral line

broadening. McCumber and Sturge[6–8] have carried out experiments on the R lines of ruby while more recently Kushida and Kikuchi[9] have extended this study to the R, R', and B' lines. Imbusch *et al.*[10] have also studied the $^2E \rightarrow {}^4A_2$ lines of Cr^{3+} and V^{2+} in MgO, but it is only recently that studies have been carried out on the rare-earth ions. Yen, Scott, and Schawlow[11] investigated the phonon-induced relaxation of Pr^{3+} in LaF_3, while Kushida[12] used Nd^{3+} to study YAG and calcium fluorophosphate. All of these investigations, except for the detailed study by Yen *et al.*, have concentrated on the Raman-type relaxation process, which is the dominant one at higher temperatures. The direct-process terms have been ignored as a temperature-dependent component process by being treated as an additional constant in the zero-point width. Our investigations show that they are necessary components of the temperature-dependent linewidth contribution and must be included if the experimentally observed temperature dependence is to be fully explained.

II. EXPERIMENTAL DETAILS

The sample used was a single crystal of YAG doped with 1% of Pr^{3+}, i.e., $Pr^{3+}_{0.03}Y^{3+}_{2.97}Al^{3+}_5O^{2-}_{12}$ with a mass of 0.2768 ± 0.0001 g and a thickness of 3.4 ± 0.1 mm. They were grown by slow cooling (2 °C/h) from the melt in the presence of an excess of PbF_2-PbO flux, in a closed platinum crucible. A temperature gradient from the top to the bottom of the crucible resulted in a few large regular crystals growing inside the melt, instead of many small ones on top. The crystal sample used in the experiment was cut and polished with two parallel sides.

The absorption spectrum was observed with the use of a Hilger-Engis Monospek 1000-grating spectrophotometer. Being a plane-grating symmetrical Czerny-Turner spectrophotometer, it had interchangeable gratings, separate fully adjustable curved slits, and a focal length of 1 m. In the visible region a CSIRO 4-in. grating was used which was blazed at 3000 Å. For the near infrared, a Bausch and Lomb 10-cm grating gave a dispersion of 16 Å/mm at a blaze wavelength of 10 000 Å.

The spectrum was recorded with an IP28 photomultiplier attached to the exit slit, connected via a Perkin Elmer 107 amplifier to a Servoscribe potentiometric chart recorder.

A liquid-nitrogen Dewar and a "Hoffman" liquid-helium cryostat were used to cool the sample to 77 and 4.2 °K, respectively. To obtain variable temperatures from 4.2 to 300 °K, two methods were employed. For temperatures near the two cold points, an Ether variable temperature regulator was used, and for higher temperatures (> 100 °K) the spectra at various temperature points were obtained by merely allowing the sample to warm up after the coolant had evaporated. In this way temperatures to within ± 1 °K could be obtained for any particular linewidth recording.

The resolution was tested using the 3131-Å Hg doublet, and was found to be better than 0.18 Å (0.7 cm^{-1} at 5000 Å).

III. THEORETICAL REVIEW

As indicated previously, phonon-induced ion-relaxation mechanisms have been used successfully to explain the observed thermal broadening of sharp optical spectra. The nature of these ion-relaxation mechanisms has long been established by Van Vleck,[13] Scott and Jeffries,[14] Yen *et al.*,[11] and many others. The following paragraphs summarize the relevant theoretical expressions and their relationship to thermal line broadening.

The Hamiltonian describing the system of an impurity ion in a host lattice is

$$\mathcal{H} = \mathcal{H}_0 + V + \mathcal{H}_p + \mathcal{H}_I \,, \tag{1}$$

where $\mathcal{H}_0$ is the free-ion Hamiltonian, V is the crystal-field potential, $\mathcal{H}_p$ is the Hamiltonian describing the phonon system, and

$$\mathcal{H}_p = \sum_k (a_k^\dagger a_k + \tfrac{1}{2})\hbar\omega_k . \tag{2}$$

$\mathcal{H}_I$ is the Hamiltonian describing the interaction between the phonon system and the ion:

$$\mathcal{H}_I = \sum_k \left(\frac{\hbar}{2Mv^2}\right)^{1/2} C\,\omega_k^{1/2}(a_k - a_k^\dagger) + \sum_{kk'} \left(\frac{\hbar}{2Mv^2}\right) D\omega_k^{1/2}\omega_{k'}^{1/2}(a_k - a_k^\dagger)(a_{k'} - a_{k'}^\dagger) + \cdots . \tag{3}$$

Therefore,

$$\mathcal{H}_I = \mathcal{H}_I' + \mathcal{H}_I'' + \cdots ,$$

where a_k and $a_k^\dagger$ are the annihilation and creation operators for phonons in the kth mode, ω_k is the frequency of the kth mode, C and D are the first- and second-order crystal-field coupling operators operating on the electronic states $|A_i\rangle$, M is the mass of the crystal, and v is the velocity of sound in the crystal ($= \omega_k/k$).

The width of a spectral line has two basic component types: an inhomogeneous width and a homogeneous component. Inhomogeneous line broadening arises primarily from random local strains in the lattice, which result in different ions in the lattice having slightly different crystal-field environments. The net result over the whole crystal is a finite temperature-independent linewidth component which, because of the randomness of its origin, produces a Gaussian line-shape component.

Together with this constant zero-point width there

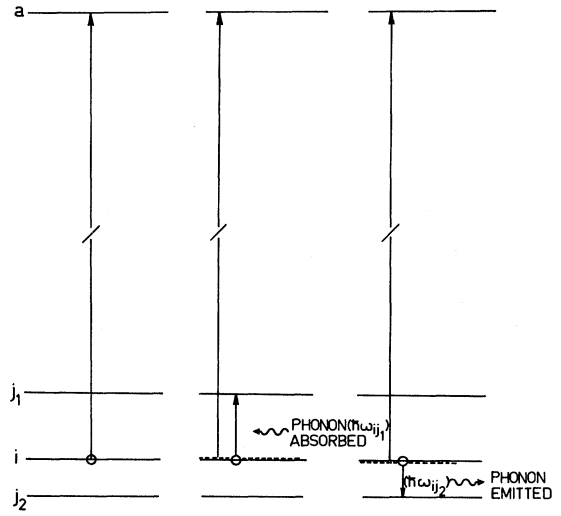

FIG. 1. Direct one-phonon relaxation processes.

is an homogeneous component which increases rapidly with temperature. This component stems from the various ion-relaxation processes which can occur in competition with the optical excitation of the ion by the absorption of a photon of light. These ion-relaxation processes are induced by the phonon system surrounding the ion, as energy transfers can take place between them. Thus ion-lattice interactions, described by the interaction Hamiltonian $\mathcal{H}_I$, allow ion-relaxation processes to occur which, through their relaxation probabilities, give rise to homogeneous temperature-dependent line-broadening effects.

Each type of ion-relaxation process has its own contributing probability which will lead to a broadening of the electronic level A_i, and hence to the broadening of the optical transition $A_i \rightarrow B$. Thus the total homogeneous linewidth component can be separated further into components corresponding to each possible relaxation mechanism, each having its own peculiar temperature dependence. The strength or magnitude of these linewidth components will depend naturally on the amount of coupling between the ion and the lattice. If the probability of an ion relaxing from its electronic state to a neighboring one is small, due either to the nature of the eigenstates involved or to the small amount of coupling between the ion and the lattice, then the linewidth of the optical transition will be narrow.

We must consider the contribution of each type of ion-relaxation process to the final total spectral linewidth.

For direct one-phonon relaxation processes, which consist of the direct absorption or emission of a phonon (see Fig. 1), the transition probability is

$$W_i^d = \frac{2\pi}{2Mv^2\hbar}\left\{\sum_{j<i}\omega_{ij}\,\rho(\omega_{ij})\,|\langle A_i|\,C\,|A_j\rangle|^2[P_0(\omega_{ij})+1] + \sum_{j>i}\omega_{ij}\,\rho(\omega_{ij})\,|\langle A_i|C|A_j\rangle|^2 P_0(\omega_{ij})\right\}$$

$$= \sum_{j<i}\pi\beta_{ij}\,[P_0(\omega_{ij})+1] + \sum_{j>i}\pi\beta_{ij}\,P_0(\omega_{ij})\,, \tag{4}$$

where $\rho(w_{ij})$ is the detailed phonon density of states at frequency ω_{ij}, and

$$P_0(\omega_{ij}) = (e^{\hbar\omega_{ij}/KT}-1)^{-1} \tag{5}$$

is the thermal phonon population of the $k(\omega_{ij})$ mode, which equals 0 at $T=0\,^\circ$K. Thus,

$$W_i^D = \sum_{j<i}\pi\beta_{ij} \quad \text{at } T=0\,^\circ\text{K}\,.$$

$\pi\beta_{ij}$ is the direct-process linewidth parameter

$$\pi\beta_{ij} = \frac{\omega_{ij}}{Mv^2\hbar}\,\rho(\omega_{ij})\,|\langle A_i|\,C\,|A_j\rangle|^2 \tag{6}$$

and is dependent on $\rho(\omega_{ij})$, M, v, the energy gap $\hbar\omega_{ij}$, and the amount of coupling between the states $|A_i\rangle$ and $|A_j\rangle$ by $\mathcal{H}_I$. Thus $\pi\beta_{ij}$ gives a direct measure of the strength of the ion-lattice interactions. The temperature dependence of this term arises only through the phonon population $P_0(\omega_{ij})$ given by (5), and at higher temperatures this approaches a direct proportionality relationship (see Fig. 8).

Multiphonon direct processes allow relaxation to states separated by an amount $\hbar\omega_{ij} > K\Theta_D$. As single phonons of this energy do not exist, relaxation can take place only by the simultaneous emission or absorption of two or more phonons (see Fig. 2). High-order perturbation theory shows that the transition probability for these processes is approximately temperature independent and negligibly small in our temperature range. Thus

$$W_i^n \simeq \text{constant } N \tag{7}$$

and

$$W_i^2 > W_i^3 > \cdots > W_i^n\,.$$

The dominant linewidth component at temperatures above 50 °K arises from Raman-type relaxation processes. These multiphonon processes can be considered classically as the scattering of a phonon by the impurity ion, in which the ion loses or gains energy from the collision to relax to a neighboring electronic state (see Fig. 3). Quantum mechanically the ion simultaneously absorbs a phonon and emits another, the difference in energy between the two phonons being the amount by which the ion is excited or relaxed (see Fig. 3). This second-order process has a transition probability

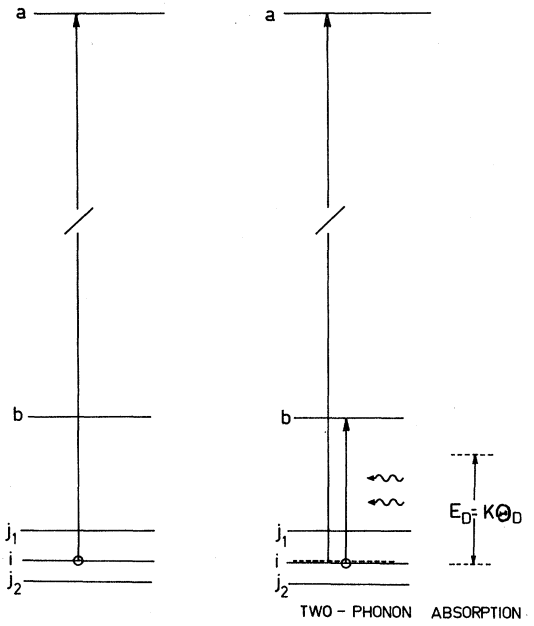

FIG. 2. Direct N-phonon relaxation processes.

W_i^R which may be calculated by applying $\mathcal{H}'$ in second order and $\mathcal{H}''$ in first order:

$$W_i^R = \frac{2\pi}{\hbar}\,\bar{\alpha}_i (T/\Theta_D)^7 \int_0^{\Theta_D/T} \frac{x^6 e^x}{(e^x-1)^2}\,dx\,, \tag{8}$$

where

$$x = \hbar\omega/KT\,,$$

$$\bar{\alpha}_i = \frac{1}{K\Theta_D}\left[\alpha_i^2 + \frac{9\hbar^2}{8\pi^4\rho^2 v^{10}}\left(\frac{K\Theta_D}{\hbar}\right)^6\left(\sum_{j\neq i}|\langle A_j|D|A_i\rangle|^2 + \sum_{i\neq j\neq k}\frac{|\langle A_j|C|A_k\rangle|^2|\langle A_k|C|A_i\rangle|^2}{E_{jk}E_{ki}}\right)\right],$$

$$\alpha_i = \frac{3\hbar}{2\pi^2\rho v^5}\left(\frac{K\Theta_D}{\hbar}\right)^4\left(\langle A_i|D|A_i\rangle - \sum_k \frac{|\langle A_k|C|A_i\rangle|^2}{E_{ik}}\right),$$

assuming a Debye phonon density of states. The integral $\xi_6(\Theta_D/T)$ in (8) has been tabulated by Ziman.[15]

Collecting these homogeneous components, which all form Lorentzian line shapes, we have, for the ith level, the total contribution to the linewidth resulting from $\mathcal{H}_I$ as

$$\Delta_i = W_i^D + W_i^n + W_i^R = \sum_{j<i}\pi\beta_{ij}\,[P_0(\omega_{ij})+1] + \sum_{j>i}\pi\beta_{ij}\,P_0(\omega_{ij}) + N + \frac{2\pi}{\hbar}\,\bar{\alpha}_i\left(\frac{T}{\Theta_D}\right)^7 \xi_6\left(\frac{\Theta_D}{T}\right). \tag{9}$$

Therefore, the total linewidth of the optical transition $i \to B$ is

$$\Delta = \Delta_i + \Delta_B + \Delta_{\text{strain}}\,. \tag{10}$$

IV. EXPERIMENTAL RESULTS

The optical transitions studied were those from the lowest triplet levels of the ground-state multiplet $^3H_4$ to the excited-state singlet level $^3P_0$. The observed energy-level scheme is illustrated in Fig. 4. The position of the $^3P_0$ level is in agreement with the previous experimental results of Hooge[16]: $20\,533.2 \pm 0.2$ cm^{-1} compared with his value of $20\,533 \pm 3$ cm^{-1}. Our values of the ground-state triplet splitting [measured at $T = 90 \pm 3$ °K] agree with his average values for all levels, but not with his particular observations for the $^3P_0$ transitions (see Table I). Measurements of the width of these three transitions were made at an absorption coefficient value of half-maximum for each line. Temperatures ranged from 7 to 300 °K. Variation of linewidth as a function of temperature is shown in Figs. 5–7. Linewidth measurements for transition II were only possible at low temperatures because of its low transition strength, which suggests that it is a $\Gamma_5(\mu=2) \to \Gamma_1(\mu=0)$ transition, forbidden in D_2 symmetry.

The theoretical linewidth curve can be obtained from Eqs. (9) and (10). The assumptions made are that, for the ith level, only interactions between levels of the ground-state triplet are included, and that, for level B, $\Delta_B = W_B^R$ only. Therefore we have

$$\Delta = \Delta_i + W_B^R + \Delta_{\text{st}}$$

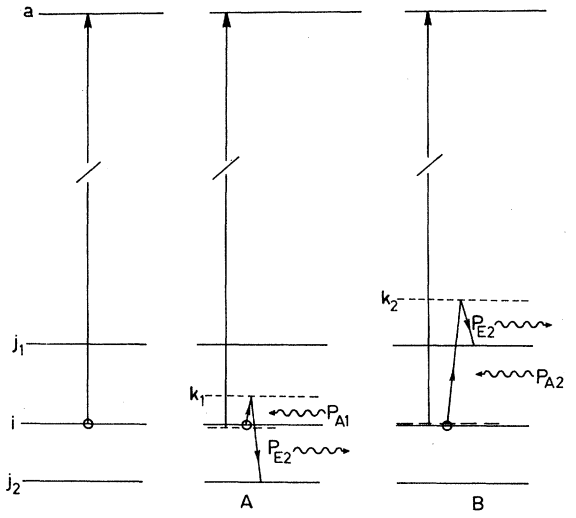

FIG. 3. Raman relaxation processes, the simultaneous absorption and emission of a phonon.

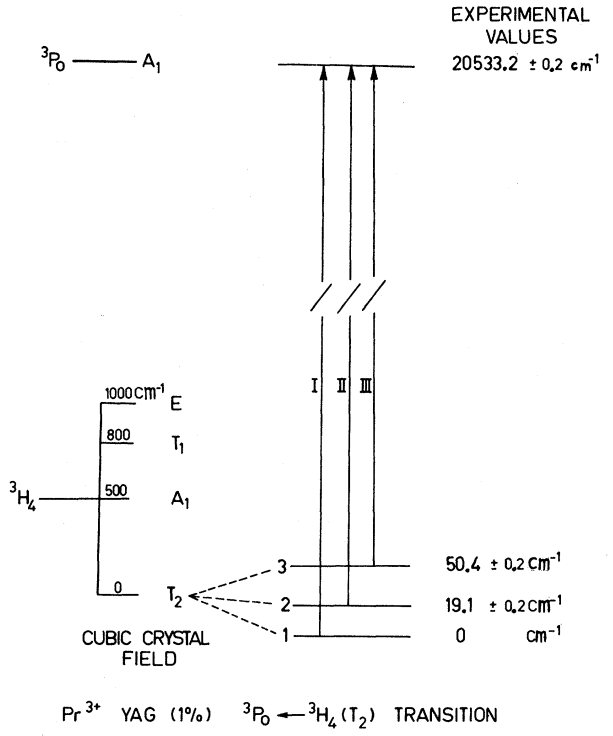

FIG. 4. Experimental energy-level scheme.

$$= W_i^D + \frac{2\pi}{\hbar}(\bar{\alpha}_i + \bar{\alpha}_B)\left(\frac{T}{\Theta_D}\right)^7 \xi_6\left(\frac{\Theta_D}{T}\right) + \Delta_{st}\,, \qquad (11)$$

with $\bar{\alpha}_B \ll \bar{\alpha}_i$ and $N \approx 0$. A Θ_D of 750 °K was taken for YAG [12] which gives $K\Theta_D \approx 520$ cm^{-1}.

The first assumption can be made because the next highest level of the ground-state manifold is about five to six hundred wave numbers away, which is greater than $K\Theta_D$ and large compared with the splittings of the triplet (~ 50 cm^{-1}). Similarly for the $^3P_0$ level, the nearest level is 200 cm^{-1} away, which means $W_B^D \simeq 0$ and $\bar{\alpha}_B$ will be very small.

From Eq. (11) the theoretical curve for transition I has the form

$$\Delta_I = \pi\beta_{12} P_0(\omega_{12}) + \pi\beta_{13} P_0(\omega_{13}) + \frac{2\pi}{\hbar}\bar{\alpha}_I\left(\frac{T}{\Theta_D}\right)^7 \xi_6\left(\frac{\Theta_D}{T}\right) + \Delta_{st}\,.$$

Using a computer program, this expression was fitted to the experimental data to obtain the line of best fit (see Figs. 5–7) and the parameters $\pi\beta_{ij}$, $\bar{\alpha}_{iB}$, and Δ_{st}. With each graph of the experimental points, the theoretical linewidth components and the total resultant linewidth have been drawn using these best-fit parameters. The parameters are tabulated in Table II for the three transitions.

TABLE I. Comparison of ground-state triplet splitting.

Expt (cm^{-1})	Hooge (Ref. 16) Av (cm^{-1})	Hooge (Ref. 16) $^3P_0$ transitions (cm^{-1})
19.1 ± 0.2	19	20
50.4 ± 0.2	50	46

The lines of best fit for transitions I, II, and III are

$$\Delta_I(T) = 1.19 + 0.10P_0(\omega_{12}) + 0.001P_0(\omega_{13}) + 334.2\left(\frac{T}{\Theta_D}\right)^7 \xi_6\left(\frac{\Theta_D}{T}\right) \text{cm}^{-1}\,,$$

$$\Delta_{II}(T) = 1.40 + 0.10[P_0(\omega_{12}) + 1] + 0.42P_0(\omega_{23}) + \left(\alpha_{II}\frac{2\pi}{\hbar}\right)\left(\frac{T}{\Theta_D}\right)^7 \xi_6\left(\frac{\Theta_D}{T}\right) \text{cm}^{-1}\,,$$

$$\Delta_{III}(T) = 0.76 + 0.001[P_0(\omega_{13}) + 1] + 0.42[P_0(\omega_{23}) + 1] + 196.5\left(\frac{T}{\Theta_D}\right)^7 \xi_6\left(\frac{\Theta_D}{T}\right) \text{cm}^{-1}\,.$$

A parameter fit could not be made for transition II because of the small number of data (Fig. 6 is a hand-drawn line of best fit). Thus a value of α_{II} could not be obtained.

Errors associated with these measurements are ± 3% in the linewidth Δ_i and ± 1 °K in the temperature measurements. A greater fluctuation of the

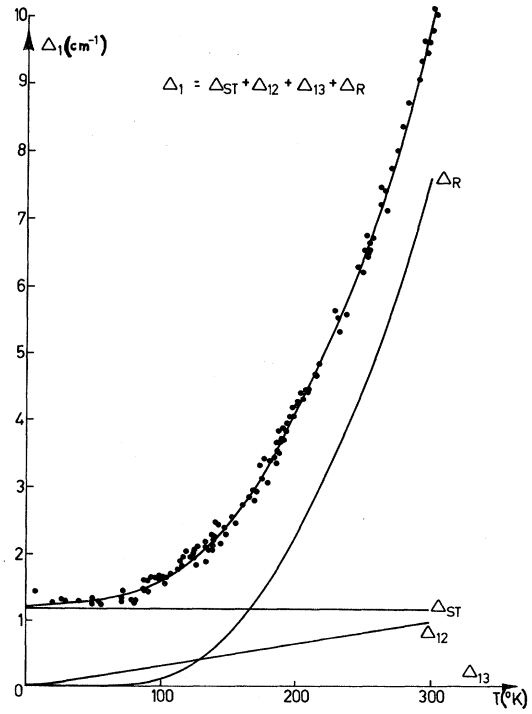

FIG. 5. Experimental and theoretical temperature variation of linewidth for transition I.

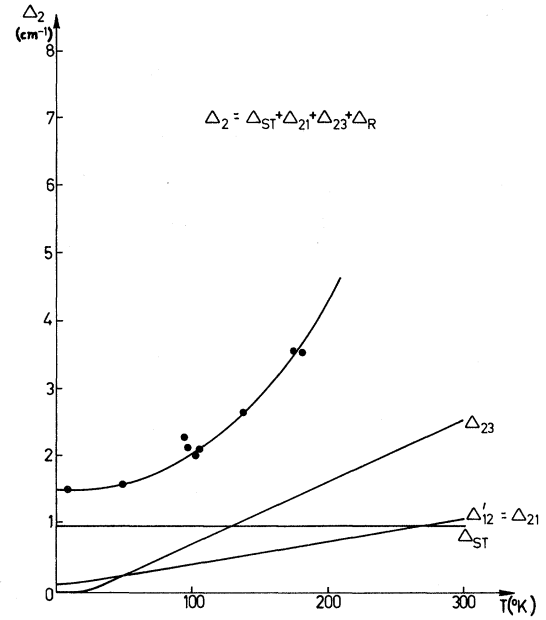

FIG. 6. Experimental and theoretical temperature variation of linewidth for transition II.

data points (Δ, T) was observed particularly at lower temperatures because of the difficulty associated with measuring the actual sample temperature. Our assumption that the thermocouple followed faithfully the temperature of the sample portion in the beam, as the temperature was varied, probably contributed to the observed scattering.

To illustrate clearly the respective T dependences of each type of relaxation-process contribution, log-log graphs have been plotted in Figs. 8–10 for transition I.

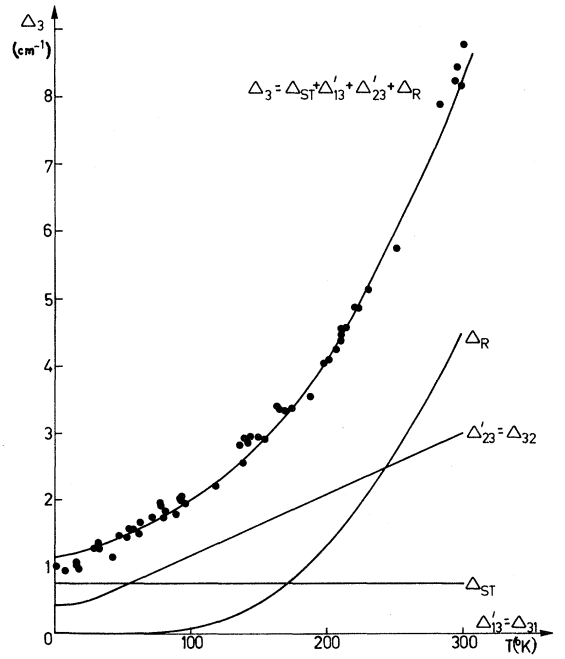

FIG. 7. Experimental and theoretical temperature variation of linewidth for transition III.

V. DISCUSSION AND INTERPRETATION

From Figs. 5–7 we can see that the theoretical linewidth expressions given above fit the experimental data quite well. The relative magnitudes of the parameters agree with the amount and type of coupling we would expect between the levels.

We find $\pi\beta_{12} \sim \pi\beta_{23}$, as we would expect from the energy-level scheme. $\pi\beta_{13} \ll \pi\beta_{12}$ and $\pi\beta_{23}$ because the separation between the two levels (1 and 3) is the largest of all. The direct relaxation process $3 \rightarrow 1$ also has a competing process $3 \rightarrow 2 \rightarrow 1$, which we would expect to have a higher probability. The two separate determinations of $\pi\beta_{13}$ both agree to an order of magnitude and give $\pi\beta_{13} \simeq 0$. This is encouraging in the light of assumptions made previously that levels with a separation greater than 200 cm^{-1} have negligible contributions to the linewidth of a particular level.

The apparent poor correlation between the values of Δ_{st} obtained for the three transitions can be explained by the high errors associated with these values, and by the removal of the assumption that Δ_{st} is independent of the levels involved. Hutchings and Wolf[4] have shown that for the garnets the values of the second-degree crystal-field parameters V_2^0 and V_2^2 are extremely sensitive to the exact position of the impurity ion, and hence to the presence of any local strains in the lattice. This could explain the relatively high values of Δ_{st} obtained, and also the observed variation with the levels involved. We would expect fluctuations in V_2^0 and V_2^2 to affect different electronic levels in quite separate ways. (See Ref. 12, p. 507.)

With the linewidth parameters $\pi\beta_{ij}$ and α_{iB} known, we should be able to obtain estimates of the matrix elements $\langle A_i | C | A_j \rangle$ and $\langle A_i | D | A_j \rangle$ by using Eqs. (6) and (8). Final determinations, however, rest on a detailed knowledge of the phonon density of

TABLE II. Linewidth parameters for the $^3H_4 \rightarrow {}^3P_0$ transitions of Pr^{3+}:YAG.

Parameter	Transition (cm^{-1}) I	II	III
Δ_{st}	1.2 ± 0.4	1.4 ± 0.4	0.8 ± 0.4
$\pi\beta_{12}$	0.10 ± 0.01		
$\pi\beta_{13}$	0.001 ± 0.0001		0.001 ± 0.001
$\pi\beta_{23}$			0.42 ± 0.01
α_1	$(5.6 \pm 0.1) \times 10^{-26}$		
α_3			$(3.3 \pm 0.1) \times 10^{-26}$

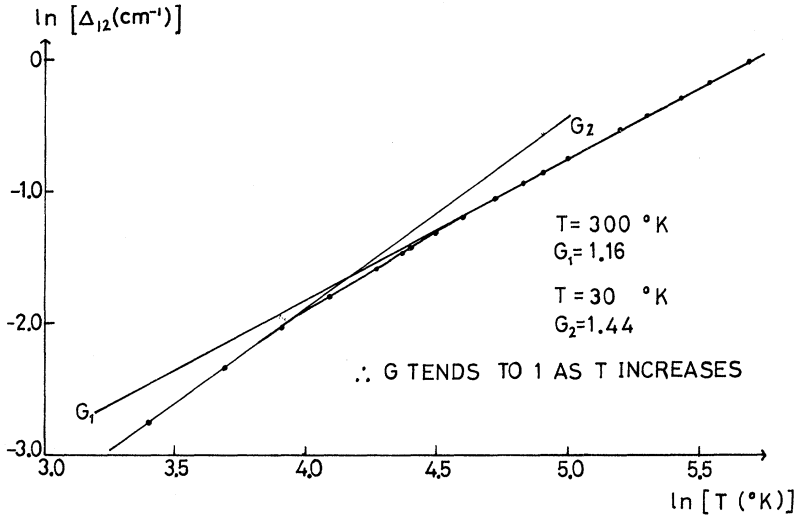

FIG. 8. Natural logarithm of the direct-process linewidth contribution plotted against ln(temperature).

states $\rho(\omega_{ij})$ at frequencies ω_{ij}. If these were obtained from the vibrational spectra surrounding the no-phonon line, using the relationships for the intensity of the sidebands given by Yen, [11] the matrix elements $\langle A_i | C | A_j \rangle$ could be determined.

It is of interest to compare the parameters obtained from our experiments with those obtained by Yen[11] for the same transitions of Pr^{3+} in LaF_3. (See Table III.) It is obvious that the direct process is a much stronger contribution to the resultant linewidth in LaF_3 than in YAG. Thus the amount of ion-lattice interaction in first order appears very small for an ion in the YAG lattice as compared with the similar interactions between the ion and the LaF_3 lattice. This tendency to behave more like a free ion when in YAG is shown even more obviously when one compares the over-all magnitudes of the linewidths at, e.g., 200 °K (see Table IV). This small ion-lattice interaction is in keeping with the general physical characteristics of the garnets and, with the resultant narrow linewidths, emphasizes the importance of rare-earth-ion–doped garnets as suitable laser materials. As Wong *et al.* [17] have shown, the Pr—F bond has a much more ionic nature than the Pr—O bond found in Pr^{3+}-doped YAG. Their conclusions were that there was a change of some 2% in the covalent character of the bonds in going through the series Pr—F, Pr—H_2O, Pr—Cl, Pr—Br, to Pr—O. This would suggest a stronger ion-lattice interaction for Pr^{3+} in LaF_3 than for Pr^{3+} in YAG, which agrees with our experimental results. Upon first glance Table II seems to indicate a large difference in the direct-process ion-lattice coefficients (a factor of 56 for $\pi\beta_{12}$). When allowance is made in Eq. 6 for the different velocities of sound (2.79 km/sec in LaF_3 and 8.58 km/sec in YAG) and for the different crystal-field energy-level splittings [$\hbar\omega_{12}(LaF_3) = 58.6$ cm^{-1} and $\hbar\omega_{12}(YAG) = 19.1$ cm^{-1}] this factor is reduced to a more reasonable value of 1.7. It can be accounted for by the stronger rare-earth-ion–lattice bonds in LaF_3 which result in a larger ion-lattice interaction, keeping in mind also that the phonon density of states $\rho(\omega_{ij})$ will probably vary from

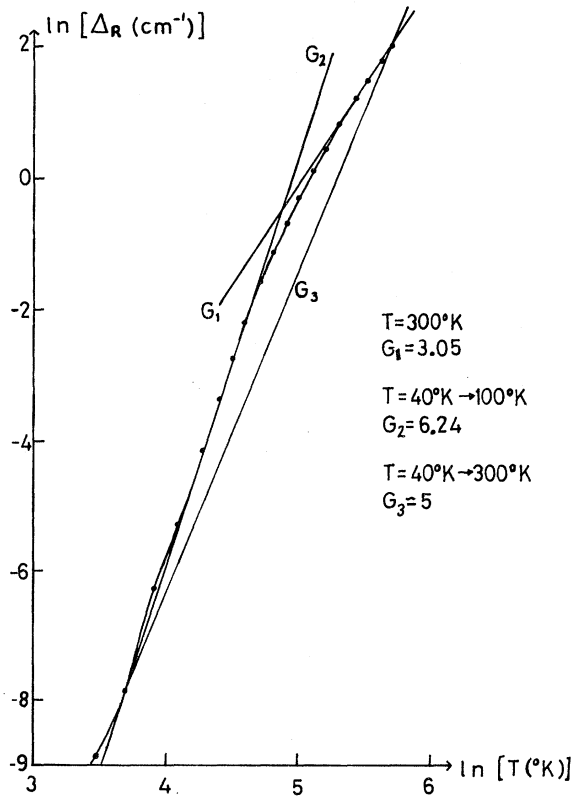

FIG. 9. Natural logarithm of the Raman process linewidth contribution plotted against ln(temperature).

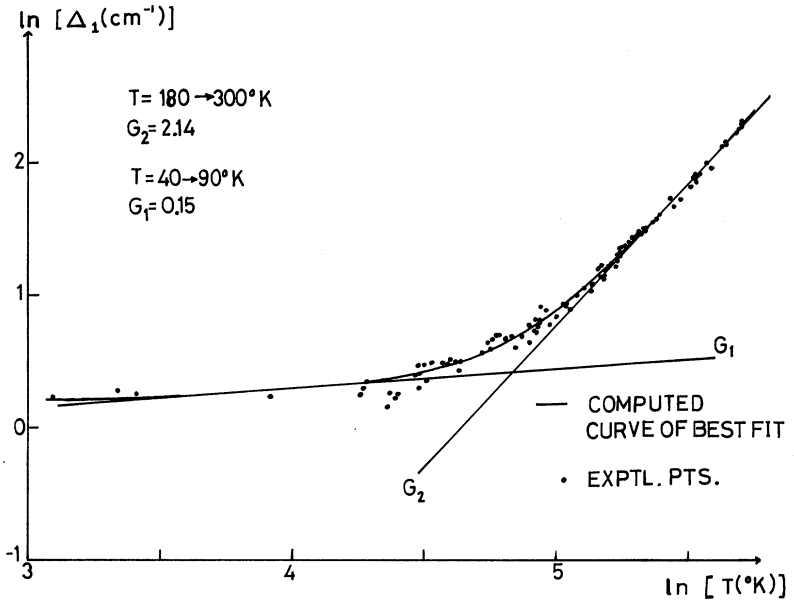

FIG. 10. Natural logarithm of the experimental linewidth and the total theoretical expression plotted against ln(temperature) for transition I.

LaF_3 to YAG.

As can be seen from Figs. 5 and 7, the Raman process has a very small contribution to the temperature-dependent linewidth below 100 °K. This means that when the direct-process coefficients $\pi\beta_{ij}$ are large, or when the energy-level separations $\hbar\omega_{ij}$ are small, the temperature dependence of the optical linewidth becomes completely dominated by the temperature dependence of the direct processes for $T < 100$ °K. This is particularly evident in the case of transition III (Fig. 7), where $\hbar\omega_{23}$ is small (31.3 cm^{-1}) and $\pi\beta_{23}$ is relatively large.

A careful study of the log-log graphs of Figs. 8–10 shows the importance of including the temperature dependence of the direct-phonon relaxation processes as contributors to the over-all linewidth temperature dependence. From Fig. 8 we see that W_i^D tends towards a direct proportionality relationship as T is increased, i.e., $W_i^D \propto T$. From Fig. 9, for the Raman process, the gradient varies from a constant value of 6.25 between 40 and 100 °K to a value of 3 at 300 °K. The over-all picture suggests a T^6 variation for most of the temperature range. Thus at low temperatures we would expect the direct processes to dominate as $W_i^D \propto T$, whereas $W_i^R \propto (T/\Theta_D)^6$ (see Figs. 5–7), but at higher temperatures the T^6 variation of the Raman term completely takes over.

Figure 10 shows the observed variation of the experimental points, together with the variation of the total theoretical expression. Once again, experiment fits theory quite well, and the resultant gradient of 0.15 at low temperatures rises to a steady 2.14 at higher temperatures, indicating two important aspects of thermal line broadening. The first is the eventual domination of the linewidth by the Raman term once its magnitude becomes comparable with that of the direct processes. The second important point is the obvious necessity to include the temperature dependence of the direct process as a contributor. If W_i^D is assumed to be temperature independent then we would expect the temperature dependence of the total linewidth to be purely due to the Raman term (i.e., T^6). In fact, its maximum variation rate is a T^2 relationship indicating the necessary summation of a T term with

TABLE III. Linewidth parameters for Pr^{3+} $^3P_0 \leftarrow {}^3H_4$ transitions.

Parameter	Lattice YAG (cm^{-1})	LaF_3 (cm^{-1})
$\pi\beta_{12}$	0.10	5.6
$\pi\beta_{13}$	0.001	0.5
$\pi\beta_{23}$	0.42	5.7
$\alpha_1 2\pi/\hbar$	334.2	200
$\alpha_3 2\pi/\hbar$	196.5	210

TABLE IV. Linewidths of $^3P_0 \leftarrow {}^3H_4$ transitions of Pr^{3+} at 200 °K.

Transition	Lattice YAG (cm^{-1})	LaF_3 (cm^{-1})	Nd^{3+} in YAG (cm^{-1})
Δ_1	4	20	~4
Δ_3	4	35	

this T^6 term. Thus an analysis which does not include the direct phonon processes as contributors to the temperature variation of the spectral linewidth could not possible hope to obtain a good correlation between theory and experiment, even if there appears superficially to be correlation.

The obvious extension of this work is to carry out a similar analysis of ion-lattice interactions in magnetic materials, to see if analogous magnon relaxation processes are observable. As the phonon system surrounding an ion provides a ready reservoir and means of ion-lattice interaction, so too should the surrounding system in a magnetic lattice. The main problem is to obtain a system in which such processes will have measurable contributions to spectral linewidths. This has been discussed in a previous paper,[18] and we hope to carry out these and related studies on the systems $RbMnF_3:Pr^{3+}$, $RbMnF_3:Co^{2+}$, and $YIG:Tb^{3+}$.

ACKNOWLEDGMENTS

The author is indebted to Dr. J. R. Chamberlain for his suggestions and help with the project, and to Dr. J. R. Pilbrow and Dr. F. Ninio for many valuable discussions. Thanks must also go to A. Vas for growing the crystals and to R. Horan and his staff for their technical assistance.

*Present address: Department of Solid State Physics, Research School of Physical Sciences, Australian National University, Canberra, Australia.

[1]H. S. Yoder and M. L. Keith, Am. Mineralogist 36, 519 (1951).
[2]S. Geller and M. A. Gilleo, J. Phys. Chem. Solids 3, 30 (1957).
[3]E. Spencer *et al.*, J. Appl. Phys. 34, 3059 (1963).
[4]M. T. Hutchings and W. P. Wolf, J. Chem. Phys. 41, 617 (1964).
[5]K. W. J. Stevens, Proc. Phys. Soc. (London) A65, 209 (1951).
[6]D. E. McCumber and M. D. Sturge, J. Appl. Phys. 34, 1682 (1963).
[7]D. E. McCumber, J. Math. Phys. 5, 221 (1964).
[8]D. E. McCumber, Phys. Rev. 133, A163 (1964).
[9]T. Kushida and M. Kikuchi, J. Phys. Soc. Japan 23, 1333 (1967).
[10]G. Imbusch, W. Yen, A. Schawlow, D. McCumber, and M. Sturge, Phys. Rev. 133, A1029 (1964).
[11]W. M. Yen, W. C. Scott, and A. L. Schawlow, Phys. Rev. 136, A271 (1964).
[12]T. Kushida, Phys. Rev. 185, 500 (1969).
[13]J. H. Van Vleck, Phys. Rev. 57, 426 (1940).
[14]P. L. Scott and C. D. Jeffries, Phys. Rev. 127, 32 (1962).
[15]J. M. Ziman, Proc. Roy. Soc. (London) A226, 436 (1954).
[16]F. N. Hooge, J. Chem. Phys. 45, 4504 (1966).
[17]E. Y. Wong, O. M. Stafsudd, and D. R. Johnston, J. Chem. Phys. 39, 786 (1963).
[18]J. R. Chamberlain and J. T. Gourley, Phys. Letters 26A, 430 (1968).

PHYSICAL REVIEW B VOLUME 5, NUMBER 1 1 JANUARY 1972

Temperature Dependence of the Electronic Structure of Solid and Liquid Copper-An NMR Study

U. El-Hanany and D. Zamir
Israel Atomic Energy Commission, Soreq Nuclear Research Centre, Yavne, Israel
(Received 12 May 1971)

The Knight shift and spin-lattice relaxation rate in copper metal were measured using pulsed-NMR methods. The temperature range of the measurements extends in the solid from room temperature to the melting point (1083 °C), and in the liquid from 875 (supercooled phase) to 1250 °C. From these measurements the temperature dependence of $\mathcal{K}(\alpha)$, the reciprocal enhancement factor of the Korringa relation, is obtained. The recent developments in the theory of exchange enhancement of the Pauli susceptibility in metals are used to interpret this temperature dependence of $\mathcal{K}(\alpha)$. Thus the temperature dependence of the band effective mass m^* and of the conduction-electron spin density at the nucleus, $\langle|\psi(0)|^2\rangle$, is derived. It is shown that these quantities are strongly influenced by s-d hybridization, and their temperature dependence is explained as being due to the volume dependence of the hybridization. Similarly, the change in both m^* and $\langle|\psi(0)|^2\rangle$ on melting is shown to be caused by the accompanying volume change, and to be only weakly influenced by loss of structure and order.

I. INTRODUCTION

In a previous paper[1] (referred to henceforth as I) we presented measurements of Knight shift K and spin-lattice relaxation T_1 in copper, both in the solid and liquid states. We have tried to explain the temperature dependence of these quantities in terms of copper band structure.